PV-1 is a component of the fenestral and stomatal diaphragms in fenestrated endothelia

Radu-Virgil Stan*, Marion Kubitza, and George E. Palade

University of California at San Diego, Division of Cellular and Molecular Medicine, La Jolla, CA 92093-0651

Contributed by George E. Palade, September 20, 1999

PV-1 is a novel endothelial protein shown by immunocytochemical tests to be specifically associated with the stomatal diaphragms of caveolae in lung endothelium. Although the highest expression levels of both mRNA and protein are in the lung, PV-1 also has been found to be expressed in other organs. Using a specific antibody to the extracellular domain of PV-1, we have extended the survey on the presence of this protein at light and electron microscope level in several rat organs. Here we show that by immunofluorescence the antibody recognizes with high specificity the endothelium of the fenestrated peritubular capillaries of the kidney and those of the intestinal villi, pancreas, and adrenals. By immunolocalization at electron microscope level, the antibody recognizes specifically the diaphragms of the fenestrae and the stomatal diaphragms of caveolae and transendothelial channels in the endothelia of these vascular beds. No signal was detected in the continuous endothelium of the heart, skeletal muscle, intestinal muscularis, or brain capillaries or the nondiaphragmed fenestrated endothelium of kidney glomeruli. Taken together, our findings define the only antigen to be localized thus far in fenestral diaphragms. They also show that the stomatal diaphragms of caveolae and transendothelial channels and the fenestral diaphragms might be biochemically related, in addition to being morphologically similar structures.

The microvascular endothelium is organized as a highly differentiated squamous epithelium whose main function is to mediate the exchanges of water, macromolecules, and small solutes between the blood plasma and the interstitial fluid. The endothelial structures implicated so far in the transendothelial transport are the caveolae, transendothelial channels, intercellular junctions, and the fenestrae (1, 3–5).

Caveolae are flask-shaped or spherical plasma membrane invaginations and associated vesicles of ≈70-nm average outer diameter that can occur singly or in chains or clusters (6, 7). In invaginated form, their membranes is in continuity layer by layer with the plasmalemma proper, and, in some microvascular beds (e.g., the continuous endothelium of the lung and the fenestrated and sinusoidal endothelia), their introits or necks are provided with a stomatal diaphragm (7).

The transendothelial channels are channels of ≈60–70-nm diameter that run across the endothelial cell. They seem to be formed by the fusion of either one caveola with both luminal and abluminal aspects of the plasmalemma or by chains of usually two to four caveolae (5, 7, 8). These channels are provided with two diaphragms (one luminal and one abluminal) only in fenestrated endothelia and not in their continuous counterparts (8).

The diaphragmed fenestrae are characteristic structural elements of all fenestrated endothelia (e.g., kidney peritubular capillaries and ascending vasa recta, capillaries of intestinal villi, pancreas, adrenal cortex, endocrine glands, and choriocapillaries of the brain and eye). They are round openings or windows cutting through the endothelial cell, have a constant diameter of 63–68 nm, and occur only in the attenuated parts of the cell, in clusters referred to as ''sieve plates'' (5, 9). In en face electron microscopic images, the fenestrae appear circular, but several studies have shown that they have an 8-fold symmetry (10, 11). The rim of the fenestra (where the abluminal plasmalemma is continuing the luminal plasmalemma) is the anchoring line for the fenestral diaphragm (5). In normal sections, the diaphragm appears as a very thin (≈5–6 nm) single-layer barrier provided with a central density or knob (5, 10). Deep-etch rapid-freeze techniques have revealed the structure of the diaphragm to be composed of radial fibrils (7-nm diameter) starting at the rim and interweaving in a central mesh (the equivalent of the central knob in orthogonal sections) (11).

Although the chemical composition of endothelial caveolae started to yield some insights (ref. 12 and, for a review on caveolae, see ref. 13), the molecular components of transendothelial channels and fenestrae remained elusive. The chemistry of these endothelial microdomains has been investigated with nonspecific ''general'' probes (charged molecules and lectins alone or in combination with various degrading enzymes), which yielded some information on the surface charge, type of molecules conferring the charge, and type of glycan antennae found on the glycoproteins and glycolipids (14, 15). No specific component of the fenestral or transendothelial channels diaphragms has been identified so far.

Taking advantage of a novel antiendothelial antibody (2), we have cloned a novel caveolar protein we named PV-1 (16). PV-1 is a type II integral membrane glycoprotein of ≈50-kDa molecular mass (≈60 kDa in glycosylated form) that forms dimers *in situ*. It has a short (27-aa) intracellular N-terminal domain, a single-span transmembrane domain, and a long (380-aa) C-terminal extracellular domain. The extracellular domain contains four N-glycosylation sites and a proline-rich region near the C terminus. The highest expression levels of both mRNA and protein are found in the lung. PV-1 has been shown to colocalize with caveolin on immunoisolated endothelial caveolae from rat lung (12) and, by immunocytochemical procedures, to be specifically associated with the stomatal diaphragms of caveolae in lung endothelium (16). The PV-1 mRNA has been found, however, to be expressed also (at much lower levels) in other organs such as kidney, liver, spleen, heart, and muscle, a fact confirmed by Western blotting only in the case of kidney, spleen, and liver (16). An immunohistochemical survey has documented the presence of PV-1 on the endothelium of peritubular capillaries in the kidney (2).

Using light and electron microscopy techniques, we have extended the survey on PV-1 localization to several rat organs. Here we show that (*i*) PV-1 is a gene product specific for endothelia from several vascular beds, (*ii*) within these endothelia, PV-1 is specifically localized at the level of the diaphragms of fenestrae, caveolar stomata, and transendothelial channels, thus being the first protein to be associated with these structures, and (*iii*) the presence of PV-1 in all these diaphragms constitutes the first indication beyond morphology (5, 7) that these structures are biochemically related.

Abbreviations: RT, room temperature; EM, electron microscope (microscopy).

*To whom reprint requests should be addressed.

The publication costs of this article were defrayed in part by page charge payment. This article must therefore be hereby marked "*advertisement*" in accordance with 18 U.S.C. §1734 solely to indicate this fact.

Materials and Methods

Materials. All general reagents were from either Sigma or Fisher unless otherwise stated.

Antibodies. A chicken polyclonal antibody raised against the last 12 aa residues of the extracellular C terminus of the rat PV-1 (anti-PV-1C polyclonal antibody) (16) was used for both immunofluorescence and immunogold labeling. Preimmune IgY was prepared as described previously in ref. 16. Rabbit anti-chicken IgY-FITC was from either The Jackson Laboratory or Sigma, and rabbit anti-chicken IgY-Au (5 nm) was from Ted Pella (Redding, CA).

Microscopy. Tissue preparation was done as in ref. 16. Briefly, the vasculature of the organ/tissue of interest was flushed [5 min, room temperature (RT)] free of blood with DMEM followed by perfusion (10 min, RT) with paraformaldehyde-lysine-sodium metaperiodate (PLP) fixative. The tissues were excised, trimmed to small blocks (1 × 1 mm for semithin frozen sections and 3 × 3 mm for immunodiffusion), fixed further (overnight, 4°C) in fresh PLP, cryoprotected (overnight, 4°C) in 2.3 M sucrose and 20% polyvinylpyrrolidone, mounted on nails, snap-frozen, and stored in liquid nitrogen.

Immunofluorescence. Semithin (≈1-μm) frozen sections of PLP fixed tissues were blocked (30 min, RT) in 1.5% cold water fish skin gelatin/0.01 M glycine in PBS, reacted with the primary antibody (1 h, RT) diluted 1:200–1:2,000 in 1.5% fish skin gelatin in PBS, washed (three times for 10 min, RT) in PBS, reacted with a FITC-conjugated reporter antibody, washed again as above, mounted under glass coverslips, and examined and photographed on a Zeiss Axiophot equipped with appropriate filters. Control experiments were carried out by either using preimmune IgY or omitting the primary antibody.

Immunogold Labeling. The localization of PV-1 at the electron microscope (EM) level was obtained by immunodiffusion, a preembedding labeling method that allows adequate sampling and better preservation of the morphology of the tissues studied as compared with labeling of ultrathin cryosections. The procedure has been described in detail (16).

Immunoblotting. Rat pancreas, intestine mucosa, adrenal glands, and kidney were freshly collected, weighed, minced, and homogenized (20 strokes; Teflon pestle-glass Thomas type BB homogenizer) in an ice-cold buffer (1:4, wt/vol) containing 25 mM Hepes (pH 7.2), 250 mM sucrose, 2 mM $MgCl_2$, and a protease inhibitors mixture (10 μg/ml each leupeptin, pepstatin, *o*-phenantrolin, and E-64 and 1 mM PMSF). The homogenate was filtered through a 53-μm nylon net and centrifuged for 15 min at 500 × *g* to yield a nuclei/cell debris pellet and a postnuclear supernatant. The latter was fractionated further by centrifugation (1 h, 4°C, 100,000 × *g*, using a TLA45 rotor) in a total membranes pellet and a cytosolic supernatant. The membranes were solubilized in 0.5% SDS in 50 mM Tris·Cl, pH 6.8, supplemented with protease inhibitors (10 μg/ml each leupeptin, pepstatin, *o*-phenantrolin, and E-64, 1 mM PMSF, and 1 mM EDTA), and the protein concentration was determined by using the bicinchoninic acid method (Pierce). The membrane proteins were separated by 8% SDS/PAGE, transferred to poly(vinylidene difluoride) membranes, and subjected to immunoblotting with the chicken anti-rat PV-1 polyclonal antibody.

Results and Discussion

Employing a specific antibody directed against the extracellular domain of PV-1 (see *Materials and Methods*), we have extended the survey on the presence of this protein at light and EM levels in several rat organs. By immunofluorescence on semithin (1- to 2-μm) cryosections (see *Materials and Methods*), the antibody recognizes with high specificity the endothelium of kidney peritubular capillaries (Fig. 1 *a* and *b*) and the fenestrated endothelium of capillaries of the intestinal villi (Fig. 1*e*), pancreas (Fig. 1 *c* and *d*), and adrenal glands (Fig. 1 *f* and *g*). No signal was detected in the continuous endothelium of the aorta, capillaries of the heart (Fig. 1 *h* and *i*), skeletal muscle, intestinal muscularis, and brain, or the nondiaphragmed fenestrated endothelium of capillaries of the kidney glomeruli (Fig. 1 *a* and *b*). Our findings are in agreement with previous reports (2) with respect to the localization of PV-1 in the endothelium of kidney peritubular capillaries. Taken together with the data in the literature, our findings clearly support the endothelial specificity of PV-1. Noteworthy, this protein is present in only a subset of microvascular endothelia such as the continuous endothelium of the lung and all fenestrated endothelia so far tested. Particularly striking is the presence of PV-1 on the endothelium of the peritubular capillaries of kidney, which is fenestrated and its fenestrae are provided with diaphragms, and its absence from the glomerular endothelium, which also is fenestrated but its fenestrae are not apertured by diaphragms. The only discrepancy regarding the localization of PV-1 is the apparent absence in skeletal muscle and heart microvascular beds. Although the PV-1 mRNA is found in both these organs, we could not detect any signal by either immunofluorescence or immunoblotting (16). This would raise several possibilities, such as protein expression under detectable levels by the assays employed, localization to restricted microdomains, or existence of different PV-1 isoforms in these tissues. Further work should answer these matters.

The PV-1-positive endothelia are known to be provided in part with caveolae and in part with fenestrae and transendothelial channels. Because the diaphragms of the two latter structures closely resemble those of caveolar stomata from a morphological point of view (5), we have employed immunogold labeling by immunodiffusion to detect the precise localization of PV-1 at the subcellular level in these endothelia. As documented in Fig. 2, by immunolocalization at the EM level, the anti-PV-1 antibody recognized specifically the diaphragms of the fenestrae (Fig. 2 *a*, *b*, *d*, *g*, *h*, and *j*–*l*), the stomatal diaphragms of the caveolae (Fig. 2 *b*, *c*, *f*, and *i*–*l*), and transendothelial channels (Fig. 2 *a*–*c* and *e*) of the endothelia of PV-1-positive vascular beds (see Fig. 2 legend). As in the case of the lung endothelium (16), the label was found on the stomatal diaphragms of most caveolae and transendothelial channels at both fronts of the endothelial cell with a higher frequency on the luminal side, probably reflecting higher accessibility from the lumen. The label was also found singly or in clusters on the majority of the fenestral diaphragms on both their luminal and abluminal side. As already stated and shown in Table 1, the majority but not all the structures mentioned were labeled, which could reflect limited access of the antibody to the epitope, limitations of the technique, or, more unlikely but nonetheless possible, chemical differences from diaphragm to diaphragm. Very little label, if any, was found on other plasmalemmal endothelial microdomains such as plasmalemma proper, coated pits, or junctional introits. No labeling could be found in control experiments, where the first antibody was either replaced with preimmune IgY or omitted.

To ascertain the presence of PV-1 in the organs/tissues investigated in this study, we performed immunoblotting by using the anti-PV-1C polyclonal antibody. As documented in Fig. 3, the antibody recognizes a single band of appropriate molecular mass (≈60 kDa in reducing conditions) in the case of adrenals and kidney. As described in the Fig. 3 legend, the expression level of PV-1 in these tissues is uneven, the signal in the adrenals being by far the highest followed, in order, by pancreas, intestinal villi, and kidney. However, at longer expo-

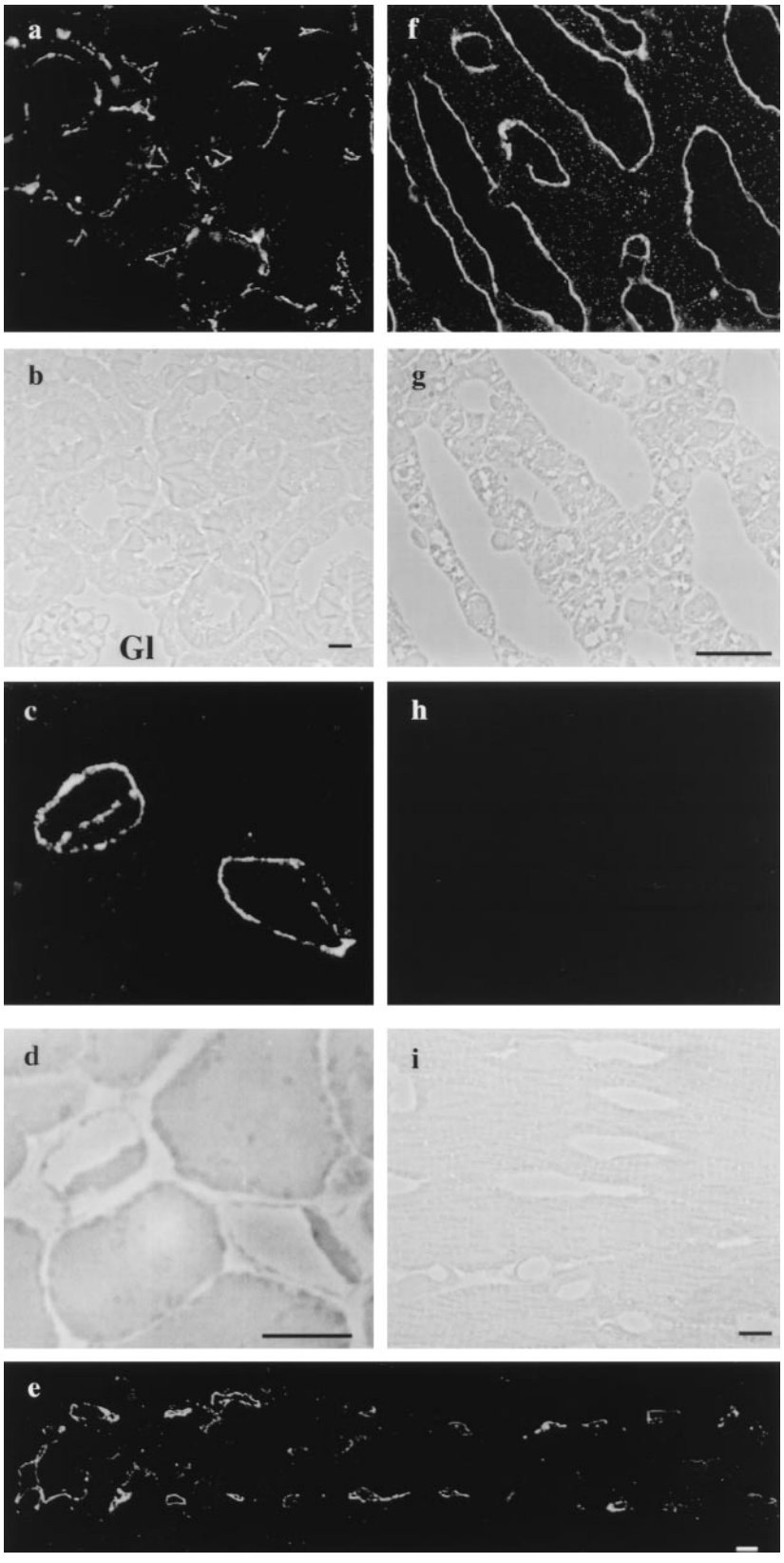

Fig. 1. Immunolocalization of PV-1 by immunofluorescence on semithin frozen section from different rat organs. Fluorescence and phase-contrast micrographs from: kidney (*a* and *b*), pancreas (*c* and *d*), intestine (*e*), adrenal glands (*f* and *g*), and heart (*h* and *i*), respectively. (*a* and *b*) The label is found specifically on the fenestrated peritubular capillaries. Please note the absence of signal from the glomerular capillaries (Gl) (where the endothelium is fenestrated but the fenestrae do not have diaphragms) or other renal structures. (*c* and *d*) An example of two labeled pancreatic acinary capillaries that shows the label on both sides of the cell. (*e*) Characteristic labeling of the fenestrated capillaries from an intestinal villus. (*f* and *g*) Labeled capillaries from the adrenal cortex. (*h* and *i*) Capillaries from the heart myocardium do not show any staining for PV-1. (Bars = 10 μm.)

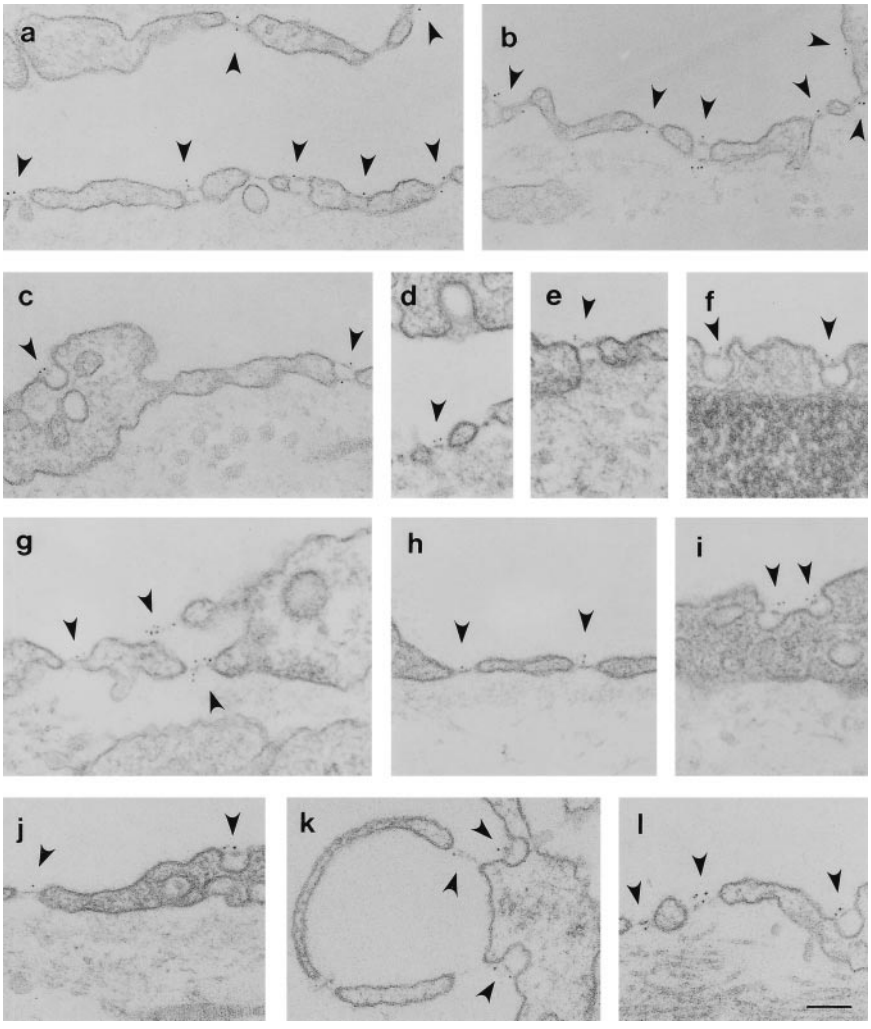

Fig. 2. Localization of PV-1 at EM level on the capillaries from kidney (*a–c*), intestine villi (*d–f*), adrenal cortex (*g*, *k*, and *l*), and pancreas (*h–j*). The respective tissues were labeled by using the anti-PV-1C polyclonal antibody followed by a 5-nm gold-conjugated reporter antibody as described in the text. Please note the labeling (arrowheads) of the stomatal diaphragms of transendothelial channels on both fronts of the endothelial cell. The fenestral diaphragms of the ''sieve plates'' or those of endothelial pockets (*k*) are labeled on both sides of the diaphragm. There is a remarkable lack of label on the proper (*a–l*), coated pits (*d*), or intercellular junctions (*a*). (Bar = 100 nm)

sure times the antibody recognizes an extra band of ≈75 kDa in pancreas and intestine (unpublished results). Further work will show whether the ≈75-kDa band is a PV-1 isoform or a protein that contains a cross-reacting epitope.

Our data provide evidence for the first antigen to be localized to fenestral diaphragms and the stomatal diaphragms of transendothelial channels, thus providing a marker and a molecular ''handle'' to be used in further studies of these structures. The localization of PV-1 offers the first indication, beyond morphology (5), that the stomatal diaphragms of caveolae and transendothelial channels and the diaphragms of the fenestrae are related structures. Last, PV-1 localization provides further evidence at the molecular level on the diversity of microvascular endothelia.

Table 1. PV-1 labeling of the diaphragms of different endothelial microdomains

	Fenestrae		Caveolae		Channels	
Organ	Counted	Labeled	Counted	Labeled	Counted	Labeled
Kidney	233	70%	72	80%	40	65%
Intestine	32	37%	76	60%	11	45%
Pancreas	59	55%	87	54%	5	20%
Adrenal gland	98	77%	16	93%	3	100%

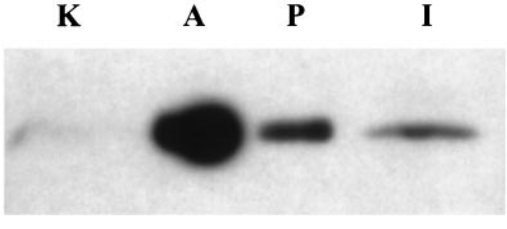

Fig. 3. Immunoblotting of different rat tissues with anti-PV-1C polyclonal antibody. Total membrane proteins from adrenals (5 μg, lane A), intestinal mucosa (100 μg, lane I), kidney (100 μg, lane K), and pancreas (10 μg, lane P) were subjected to immunoblotting, and the signal was revealed by enhanced chemiluminescence. The reason for the uneven loading was the high level of expression of PV-1 in adrenals and pancreas on one side and the low level in intestinal mucosa and kidney on the other side; as determined by preliminary experiments, the signal in adrenal glands and pancreas would interfere with the signal in the other tissues when equal amounts of protein were loaded.

That all these endothelial microdomains have been involved in transendothelial transport, correlated with the evidence presented here and data in the literature (16), would suggest a putative "sieving" function for this molecule by its participation in the formation of the diaphragms. The analysis of the PV-1 primary sequence would suggest this glycoprotein to be a component of the radial "spokes" described by scanning EM (11). Indeed PV-1 could be anchored in the membrane at the level of the rim of the fenestra and participate in protein–protein interactions via the proline-rich region situated next to its C terminus perhaps at the level of the "central knob." Whether this is the only protein participating in the formation of these diaphragms is a matter under current investigation. This would be important for the elucidation of the precise molecular mechanism of endothelial permeability in fenestrated endothelia. This could serve for further studies on the regulation of these structures, which were already shown to be modulatable in surface density by both pathological (17–24) and physiological (22–25) conditions or agents.

We thank Drs. B. Jacobson and L. Ghitescu for helpful discussions. This work was supported by National Institutes of Health Grant HL17080 to G.E.P.

1. Milici, A. J., Watrous, N. E., Stukenbrok, H. & Palade, G. E. (1987) *J. Cell Biol.* **105,** 2603–2612.
2. Ghitescu, L. D., Crine, P. & Jacobson, B. S. (1997) *Exp. Cell Res.* **232,** 47–55.
3. Simionescu, N., Siminoescu, M. & Palade, G. E. (1975) *J. Cell Biol.* **64,** 586–607.
4. Simionescu, N., Simionescu, M. & Palade, G. E. (1978) *Microvasc. Res.* **15,** 17–36.
5. Clementi, F. & Palade, G. E. (1969) *J. Cell Biol.* **41,** 33–58.
6. Palade, G. E. (1953) *J. Appl. Phys.* **24,** 1424.
7. Bruns, R. R. & Palade, G. E. (1968) *J. Cell Biol.* **37,** 244–276.
8. Milici, A. J., L'Hernault, N. & Palade, G. E. (1985) *Circ. Res.* **56,** 709–717.
9. Friederici, H. H. (1969) *J. Ultrastruct. Res.* **27,** 373–375.
10. Maul, G. G. (1971) *J. Ultrastruct. Res.* **36,** 768–782.
11. Bearer, E. L. & Orci, L. (1985) *J. Cell Biol.* **100,** 418–428.
12. Stan, R. V., Roberts, W. G., Predescu, D., Ihida, K., Saucan, L., Ghitescu, L. & Palade, G. E. (1997) *Mol. Biol. Cell* **8,** 595–605.
13. Anderson, R. G. (1998) *Annu. Rev. Biochem.* **67,** 199–225.
14. Simionescu, M., Simionescu, N., Silbert, J. E. & Palade, G. E. (1981) *J. Cell Biol.* **90,** 614–621.
15. Simionescu, N., Simionescu, M. & Palade, G. E. (1981) *J. Cell Biol.* **90,** 605–613.
16. Stan, R. V., Ghitescu, L., Jacobson, B. S. & Palade, G. E. (1999) *J. Cell Biol.* **145,** 1189–1198.
17. De Brito, T., Böhm, G. M. & Yasuda, P. H. (1979) *J. Pathol.* **128,** 177–182.
18. Hadjiisky, P. & Peyri, N. (1982) *Atherosclerosis* **44,** 181–199.
19. Suzuki, Y. (1969) *Lab. Invest.* **21,** 304–308.
20. Kitchens, C. S. & Weiss, L. (1975) *Blood* **46,** 567–578.
21. Kawanami, O., Matsuda, K., Yoneyama, H., Ferrans, V. J. & Crystal, R. G. (1992) *Acta Pathol. Jpn.* **42,** 177–184.
22. Lombardi, T., Montesano, R., Furie, M. B., Silverstein, S. C. & Orci, L. (1988) *J. Cell Sci.* **91,** 313–318.
23. Lombardi, T., Montesano, R., Furie, M. B., Silverstein, S. C. & Orci, L. (1986) *J. Cell Biol.* **102,** 1965–1970.
24. Lombardi, T., Montesano, R. & Orci, L. (1987) *Eur. J. Cell Biol.* **44,** 86–89.
25. Apkarian, R. P. & Curtis, J. C. (1986) *Scann. Electron Microsc.* **78,** 1381–1393.